

## Measuring population abundances

The population abundance of each species in each microcosm was measured once a week until 25 days after the last introduction. Twenty-five days corresponds to roughly 30 generations of the protozoa and rotifer species. Densities were estimated by counting protozoa and rotifers in samples of known volume, typically 0.3 ml, from the 3 ml of medium removed for nutrient replacement. When species were too abundant to count reliably, the sample was diluted. When one or more species were absent from the 0.3-ml sample, the entire 3 ml of medium (and the entire microcosm on the last sampling occasion) was scanned and protozoa and rotifers were counted.

## Productivity–diversity relationships

When  $P > 0.0125$  (that is,  $0.05/4$ , using a Bonferroni correction to retain a Type I error rate of 0.05) for all models (see model description in text), we concluded that the relationship between productivity and diversity was not significant. When  $P < 0.0125$  for more than one model, we selected as the best model the one that had the highest value of adjusted  $R^2$ . Adjusted  $R^2$  values are adjusted for the number of parameters in the models. When model 2 or 4 was selected, we determined whether the relationship was hump-shaped or U-shaped by using Mitchell-Olds & Shaw's test<sup>30</sup> (see Supplementary Information). We focused on the diversity of protozoan and rotifer species; our diversity index does not include bacteria, microflagebrates or algae. Productivity–diversity relationships depended on assembly history when species richness (number of species per unit volume), rather than the complement of Simpson's index, was also used to express species diversity (see Supplementary Information).

## Response of species

We conducted analyses of variance to test for effects of introduction sequence on species abundance at each productivity level. Abundance was transformed as  $\log_{10}(\text{individuals per ml} + 1)$  before analysis to minimize heteroscedasticity. For each species we used a sequential Bonferroni correction for the five tests corresponding to the five productivity levels to preserve a Type I error rate of 0.05. When analyses of variance found a significant effect of sequence, Tukey's studentized range tests were used to identify which treatments differed.

Received 18 March; accepted 8 May 2003; doi:10.1038/nature01785.

1. Waide, R. B. *et al.* The relationship between productivity and species richness. *Annu. Rev. Ecol. Syst.* **30**, 257–300 (1999).
2. Morin, P. J. Biodiversity's ups and downs. *Nature* **406**, 463–464 (2000).
3. Huston, M. A. *Biological Diversity: The Coexistence of Species on Changing Landscapes* (Cambridge Univ. Press, 1994).
4. Kondoh, M. Unifying the relationships of species richness to productivity and disturbance. *Proc. R. Soc. Lond. B* **268**, 269–271 (2001).
5. Worm, B. *et al.* Consumer versus resource control of species diversity and ecosystem functioning. *Nature* **417**, 848–851 (2002).
6. Leibold, M. A. *et al.* Species turnover and the regulation of trophic structure. *Annu. Rev. Ecol. Syst.* **28**, 467–494 (1997).
7. Kassen, R. *et al.* Diversity peaks at intermediate productivity in a laboratory microcosm. *Nature* **406**, 508–512 (2000).
8. Currie, D. J. Energy and large-scale patterns of animal- and plant-species richness. *Am. Nat.* **137**, 27–49 (1991).
9. Wright, D. H., Currie, D. J. & Maurer, B. A. in *Species Diversity in Ecological Communities: Historical and Geographical Perspectives* (eds Ricklefs, R. & Schluter, D.) 66–74 (Univ. Chicago Press, 1993).
10. Abrams, P. A. Monotonic or unimodal diversity–productivity gradients: What does competition theory predict? *Ecology* **76**, 2019–2027 (1995).
11. Gross, K. L. *et al.* Patterns of species density and productivity at different spatial scales in herbaceous plant communities. *Oikos* **89**, 417–427 (2000).
12. Scheiner, S. M. *et al.* Species richness, species–area curves and Simpson's paradox. *Evol. Ecol. Res.* **2**, 791–802 (2000).
13. Mittelbach, G. G. *et al.* What is the observed relationship between productivity and diversity? *Ecology* **82**, 2381–2396 (2001).
14. Chase, J. M. & Leibold, M. A. Spatial scale dictates the productivity–biodiversity relationship. *Nature* **416**, 427–430 (2002).
15. Gilpin, M. E. & Case, T. J. Multiple domains of attraction in competition–communities. *Nature* **261**, 40–42 (1976).
16. Post, W. M. & Pimm, S. L. Community assembly and food web stability. *Math. Biosci.* **64**, 169–192 (1983).
17. Drake, J. A. Community–assembly mechanics and the structure of experimental species ensemble. *Am. Nat.* **137**, 1–26 (1991).
18. Wilson, D. S. Complex interactions in metacommunities, with implications for biodiversity and higher levels of selection. *Ecology* **73**, 1984–2000 (1992).
19. Law, R. & Morton, R. D. Alternative permanent states of ecological communities. *Ecology* **74**, 1347–1361 (1993).
20. Connell, J. H. & Orias, E. The ecological regulation of species diversity. *Am. Nat.* **98**, 399–414 (1964).
21. Leigh, E. G. Jr On the relationship between productivity, biomass, diversity and stability of a community. *Proc. Natl Acad. Sci. USA* **53**, 777–783 (1965).
22. Pianka, E. R. Latitudinal gradients in species diversity: a review of concepts. *Am. Nat.* **100**, 33–46 (1966).
23. Rosenzweig, M. L. Species diversity gradients: We know more and less than we thought. *J. Mammal.* **73**, 715–730 (1992).
24. Rosenzweig, M. L. *Species Diversity in Space and Time* (Cambridge Univ. Press, 1995).
25. Tilman, D. & Pacala, S. in *Species Diversity in Ecological Communities: Historical and Geographical Perspectives* (eds Ricklefs, R. & Schluter, D.) 13–25 (Univ. Chicago Press, 1993).
26. Van de Koppel, J. *et al.* Patterns of herbivory along a productivity gradient: An empirical and theoretical investigation. *Ecology* **77**, 736–745 (1996).
27. Holt, R. D. & Polis, G. A. A theoretical framework for intraguild predation. *Am. Nat.* **149**, 745–764 (1997).

28. Chase, J. M. Food web effects of prey size refugia: Variable interactions and alternative stable equilibria. *Am. Nat.* **154**, 559–570 (1999).
29. Simpson, E. H. Measurement of diversity. *Nature* **163**, 688 (1949).
30. Mitchell-Olds, T. & Shaw, R. E. Regression analysis of natural selection: Statistical inference and biological interpretation. *Evolution* **41**, 1149–1161 (1987).

Supplementary Information accompanies the paper on [www.nature.com/nature](http://www.nature.com/nature).

**Acknowledgements** We thank members of the Morin laboratory for discussion, and J. A. Drake, C. M. K. Kaunzinger, M. A. Leibold, Z. T. Long, P. B. Rainey and D. Simberloff for comments. The National Science Foundation and the Department of Ecology and Evolutionary Biology at the University of Tennessee supported this research.

**Competing interests statement** The authors declare that they have no competing financial interests.

**Correspondence** and requests for materials should be addressed to T.F. (tfukami@utk.edu).

## The role of neuronal identity in synaptic competition

Narayanan Kasthuri & Jeff W. Lichtman

Department of Anatomy and Neurobiology, Washington University School of Medicine, St Louis, Missouri 63110, USA

In developing mammalian muscle, axon branches of several motor neurons co-innervate the same muscle fibre. Competition among them results in the strengthening of one and the withdrawal of the rest<sup>1,2</sup>. It is not known why one particular axon branch survives or why some competitions resolve sooner than others<sup>3</sup>. Here we show that the fate of axonal branches is strictly related to the identity of the axons with which they compete. When two neurons co-innervate multiple target cells, the losing axon branches in each contest belong to the same neuron and are at nearly the same stage of withdrawal. The axonal arbor of one neuron engages in multiple sets of competitions simultaneously. Each set proceeds at a different rate and heads towards a common outcome based on the identity of the competitor. Competitive vigour at each of these sets of local competitions depends on a globally distributed resource: neurons with larger arborizations are at a competitive disadvantage when confronting neurons with smaller arborizations. An accompanying paper tests the idea that the amount of neurotransmitter released is this global resource<sup>4</sup>.

A central feature of mammalian neural development is the reapportionment of synaptic contacts such that neurons progressively innervate fewer postsynaptic cells but with more synapses<sup>5–7</sup>. Synapse elimination at the skeletal neuromuscular junction is currently the best studied of all such rearrangements and viewed by some as a model for changes that occur in the developing brain. In the neuromuscular system of neonatal rodents, the number of muscle fibres contacted by one motor neuron decreases during the first two postnatal weeks until each muscle fibre is innervated by only one axon<sup>8</sup>. Within the arbor of a single motor axon, this branch withdrawal is protracted and asynchronous; after some terminal branches have definitively won or lost at some neuromuscular junctions, other branches of the same neuron still share synaptic sites with other innervating axons<sup>3</sup>. Several lines of evidence suggest that competitions between axon branches underlie this process<sup>9,10</sup>. It is not known, however, what properties of an axonal branch or its environment determine its destiny in these competitions. Here, we ask whether the competitive vigour of each axon branch is determined by local factors or rather is set by a global property of the parent neuron. If axonal branches were acting as agents of their

parent neurons, then synapse withdrawal should be influenced by the neuronal identities of competing axonal branches. To test this idea, we asked the following question (shown diagrammatically in Fig. 1a): when the same two axons co-innervate multiple post-synaptic cells, is the outcome skewed in favour of the same axon at all common targets?

We bred together transgenic mice that expressed either yellow or cyan fluorescent proteins (YFP or CFP) in a small, random subset of motor neurons<sup>11</sup> to create double-subset-expressing mice (see Methods). We screened approximately 200 mice between postnatal day seven (P7) and P9, to find seven limb muscles containing both a CFP- and YFP-expressing axon that co-innervated multiple neuromuscular junctions (muscles I–VII, Fig. 2). High-resolution confocal reconstructions (Fig. 1b) of the axonal branching pattern and the postsynaptic sites containing acetylcholine receptors were combined into a large montage that provided both the complete branching pattern of each motor axon and the deployment of each axon's terminals at the co-innervated junctions (Fig. 1c).

In the example shown in Fig. 1c, the CFP- and YFP-labelled axons ramified over nearly the same large portion of this muscle's multiple endplate bands and co-innervated ~1% (that is, 12) of the muscle fibres in this muscle (I, Fig. 2; see also Fig. 1c). Given the ages examined in this study (P7–P9), most of these multiply innervated muscle fibres were likely contacted by only the two labelled axons<sup>9</sup>. There was no suggestion either in terms of location in the muscle (Fig. 1c) or location within the branching tree of each axon (Supplementary Fig. 1a, b) that these axon branches or the muscle

fibres they co-innervated were exceptional.

However, by two separate criteria, the innervation of the co-innervated junctions was dramatically biased in favour of the CFP axon (Fig. 3a–h). First, the YFP axon occupied on average  $15 \pm 4\%$  ( $n = 12$ ) of the acetylcholine receptor (AChR) territory of the co-innervated neuromuscular junctions, whereas all of the CFP-expressing branches occupied more than 50% (average CFP occupation  $76 \pm 3\%$ ,  $P < 0.0001$ , Mann–Whitney test, Fig. 3i; column a, Fig. 2), a  $5.7 \pm 1.1$ -fold difference in average area of occupation. Second, the mean YFP axon calibre was about half the calibre of CFP axon branches innervating the same junctions ( $0.55 \pm 0.11 \mu\text{m}$  versus  $1.2 \pm 0.15 \mu\text{m}$ ,  $n = 12$ ,  $P < 0.03$ , Mann–Whitney test, Fig. 3j). Axons that withdraw from sites of synaptic competition become thinner than their competitor<sup>3</sup>. These results suggest that at each co-innervated junction, competition favoured the CFP axon.

Analysis of the entire set of terminal branches of these two motor axons (that is, their motor units) showed that both had a similar wide range of occupied territories and axon calibres (Fig. 3k–n), ruling out the possibility that the YFP axon generally occupied smaller synaptic territories and its branches had smaller axon calibres than the CFP axon. In addition, the junctions co-innervated by the two axons were equally likely to be contacted by a more proximal branch of the CFP axon as contacted by a more proximal branch of the YFP axon (Supplementary Fig. 1c), ruling out a systematic difference between the branch order of the two axons that co-innervated common junctions. Finally, a Monte Carlo analysis<sup>12</sup> of the sizes and areas of all 120 branches of the YFP axon showed that, within the YFP motor unit itself, the skewing towards smaller synaptic territories ( $P < 0.006$ , column b, Fig. 2) and calibres ( $P < 0.02$ ) at the cohort of junctions co-innervated by the CFP axon was highly unlikely to be a chance event.

Similar results were found in muscles III, VI and VII, where the full motor units of two labelled axons were analysed, and in muscles II, IV and V in which the thickness of the muscle restricted our analysis to superficial regions where both labelled axons were optically accessible (Fig. 2). It was unlikely that the expression of fluorescent proteins in itself had any effect on these results because in two cases (muscles I and V) the CFP axon dominated and in two cases (muscles II and III) the YFP axon dominated (compare Figs 3a–h and 4a; see also ref. 19).

The similarity of innervation patterns at the cohort of neuromuscular junctions co-innervated by the same pair of motor neurons also extended to situations with no clear skewing. In these cases (motor units 5 versus 6, 8 versus 9, 10 versus 11, and 15 versus 16, Fig. 2; see also Supplementary Fig. 2a–c) two labelled inputs segregated to opposite sides of each co-innervated junction<sup>13</sup> and on average neither had a significantly larger area (Fig. 2). The respective areas of synaptic contact at the co-innervated junctions were, however, significantly skewed relative to the rest of their motor units (column b, Fig. 2).

Two examples (muscle II and III) provided evidence that the final outcome of the competition was also strongly biased by the identity of the competitors. In these cases the weaker axon had either already lifted off the neuromuscular junction (Fig. 4a) or was a detached retraction bulb that had pulled back from the junction (see Supplementary Fig. 2f, g), even though on many other muscle fibres this same axon was the dominant branch when confronting different competitors (column b, Fig. 2). Thus the outcome of synaptic competitions for the branches of a particular axon was regulated by the company they keep, that is, the identity of the neuronal competitors.

One case appeared to provide a glimpse of a competitive hierarchy among axons. In muscle III, there were three distinctly labelled motor axons ('A', 'B' and 'C') that produced three stereotyped pair-wise sets of connections (summarized in Fig. 4b and Supplementary Fig. 2) in which axon A was dominant over B, B was equally matched by C, and A was dominant over C.

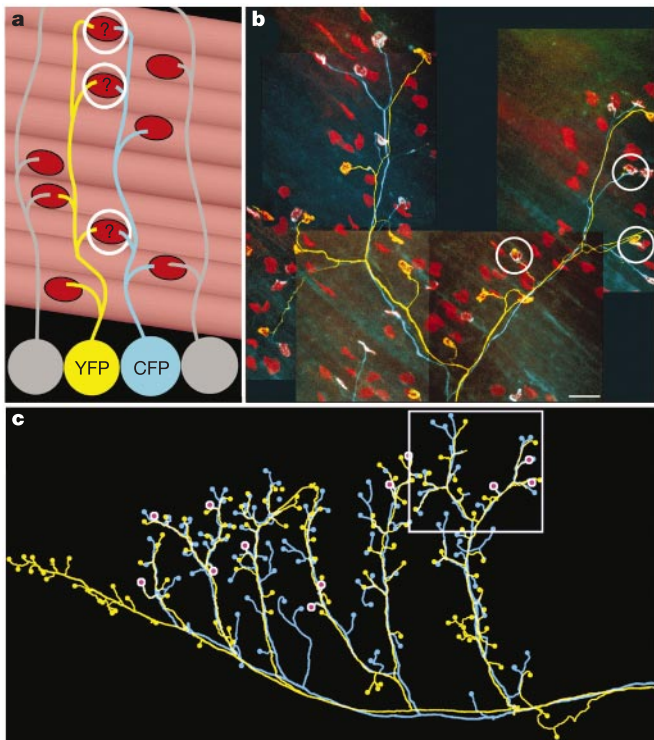


**Figure 1** Reconstructions of two competing motor units in a developing muscle. **a**, Mice were bred to generate both a single CFP- and a YFP-expressing motor axon in the same muscle. The aim was to evaluate their relative contribution to co-innervated neuromuscular junctions (circles). **b**, A montage of confocal image stacks showing the CFP (blue) and YFP (yellow) axons in one region of the flexor digitorum profundus muscle (P8). Post-synaptic receptor sites are labelled with Alexa-594 conjugated bungarotoxin (BTX-red). Co-innervated junctions are circled. **c**, Drawing of the entire CFP (blue) and YFP (yellow) motor units. The neuromuscular junctions innervated by the YFP motor unit (yellow dots), the CFP motor unit (blue dots) or both ( $n = 12$ , purple dots) are widely distributed throughout the muscle. The boxed region is shown at high resolution in **b**. Scale bar,  $50 \mu\text{m}$ .

Muscle (age)	MU	Label	MU size (number of muscle fibres)	Average synaptic occupancy (entire MU)	Number of co-innervated junctions	Outcome	a		b	
							Average synaptic occupancy (co-innervated junctions)	<i>P</i> <	Monte Carlo simulation probability ( <i>P</i> <)	
I. Flexor digitorum profundus (P9)	1	CFP	102	64 ± 8%	12		76 ± 3%	0.0001	0.003	
	2	YFP	120	65 ± 3%	12		15 ± 4% (yellow)		0.006 (yellow)	
II. Pronator teres (P8)	3	CFP	36	57 ± 7	3		8 ± 2%	0.01	0.005	
	4	YFP	23†	44 ± 4	3		98 ± 1% (yellow)		0.004 (yellow)	
III. Flexor carpi radialis (P8)	5	CFP	70	66 ± 4	3 (5 versus 6)		46 ± 2%	0.35	0.0005	
	6	brYFP	72	48 ± 3	3 (5 versus 7)		50 ± 3%		0.01	
	7	dYFP	12†	57 ± 2	3 (5 versus 7)		13 ± 2%	0.05	0.002	
					2 (6 versus 7)		0%		0.005 (yellow)	
IV. Extensor carpi ulnaris (P7)	8	CFP	20†	72 ± 8	3		44 ± 6%	0.38	0.03	
	9	YFP	26†	52 ± 9	3		41 ± 2%		0.02 (yellow)	
V. Palmaris longus (P9)	10	CFP	40†	62 ± 6	5 (10 versus 11)		40 ± 7%	0.15	0.01	
	11	brYFP	33†	74 ± 4	6 (10 versus 12)		58 ± 4% (yellow)		0.002 (yellow)	
	12	dYFP	46†	69 ± 5	6 (10 versus 12)		87 ± 5%		0.005	
VI. Extensor carpi ulnaris (P9)	13	CFP	92	64 ± 7	5		13 ± 9%	0.02	0.001	
	14	YFP	77	61 ± 5	5		85 ± 3% (yellow)		0.01 (yellow)	
VII. Flexor carpi radialis (P8)	15	CFP	78	61 ± 8	3		53 ± 4%	0.27	0.03	
	16	YFP	79	58 ± 5	3		51 ± 3% (yellow)		0.002 (yellow)	

Figure 2 Double-coloured motor units in neonatal mice. MU, motor units; \*, triply innervated junction; †, partial motor unit reconstructed.

Interestingly, the pecking order of competitors corresponded to the relative sizes of their motor axon arborizations. In four cases (muscles I, III, VI and VII) with complete motor unit reconstructions, there was an inverse relation between competitive vigour at co-innervated neuromuscular junctions and the motor unit size of the two competing axons (Fig. 4c). In these cases, the axon with the larger motor unit occupied less synaptic territory at co-innervated postsynaptic targets than the axon with the smaller motor unit. Additionally, in cases where the two motor units were equivalent in size, their branches to co-innervated junctions were equivalent in terms of occupancy. These results argue that the relative amount of some resource skews the competitive vigour in favour of the smaller axonal arbor.

In conclusion, our results show that both the pace and outcome of synapse elimination are determined by the identity of the particular inputs co-innervating a target cell. Previous work has shown that during the process of synapse elimination the various branches of a motor axon undergo retraction from muscle fibres in an asynchronous fashion<sup>3</sup>. The studies presented here show, however, that each motor axon's branches can be subdivided into several different 'cohorts'. These cohorts are distinguished by the particular identity of the competing axon at co-innervated junctions and by

the fact that axonal branch appearance and fate within each cohort appears nearly identical. The similarity of axon branch behaviour when the competing axon is the same strongly suggests that stochastic or local factors play hardly any role in determining which axon branches ultimately survive. Moreover, the fact that the branches that confront a particular competitor appear so similar argues that the temporal aspects of synapse rearrangement are highly stereotyped. The asynchrony of branch trimming in a single motor unit<sup>3</sup> thus appears to be the composite result of a series of highly synchronous synaptic reorganizations, each resolving at a different rate.

The similar appearance of the cohort of axonal branches that co-innervate postsynaptic cells shared by one other particular axon offers a unique view of many neuromuscular junctions at nearly the same stage of competition. In this way stages not previously recognized are now evident (see Supplementary Fig. 2).

These results may also provide insight into the factors that drive synaptic competition. Numerous experiments have shown that changes in synaptic activity can affect synapse competition<sup>14</sup>, and the relative activity of different synapses may be the crucial property that drives competition<sup>4,15</sup>. By the second postnatal week, when pairs of axons typically innervate the same postsynaptic cell, it is

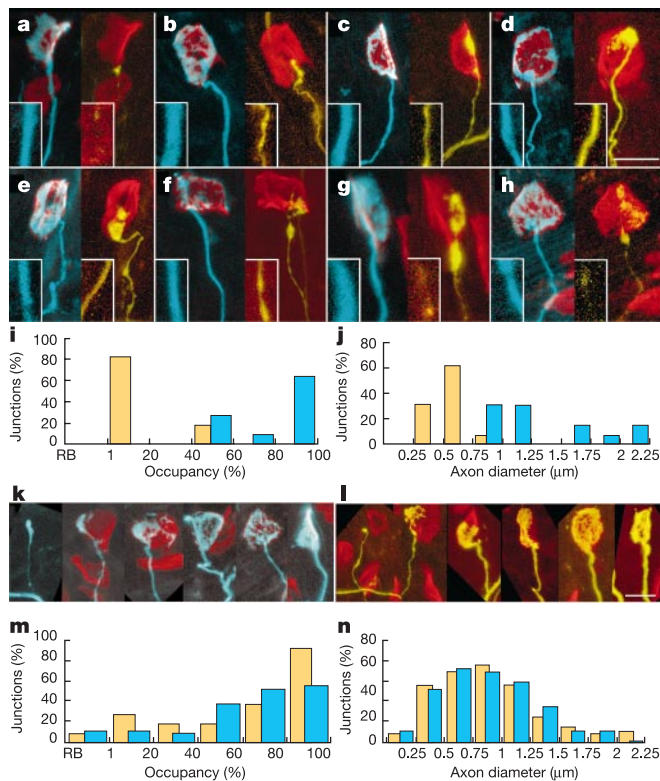


**Figure 3** Cohort of junctions co-innervated by the same two motor units are all similarly innervated. **a–h** Eight junctions co-innervated by the same CFP (left) and YFP axons (right) shown in Fig. 1. The CFP axon occupies more AChR area (red) than the YFP-expressing axon at each junction. Insets, higher-magnification views of the CFP and YFP axon calibres 10  $\mu\text{m}$  from the junctions show that the CFP axon branches are thicker than the YFP branches to the same junctions. **i**, Histogram showing the difference in synaptic occupancy between the CFP (blue bars) and YFP (yellow bars) axons at all the co-innervated junctions ( $n = 12$ ). RB, retraction bulb. **j**, Histogram showing differences in the axon calibres of the CFP and YFP axons. **k, l**, Synaptic contacts made by other branches of this CFP (**k**) and YFP (**l**) axon vary widely in neuromuscular junction occupancy. Shown is every twentieth junction for the CFP and YFP motor units ranked from smallest (left, retraction bulb) to largest (right,  $\sim 100\%$  occupation and large axon calibre). **m**, Histogram of synaptic occupancy for all junctions in each motor unit (yellow, YFP axon; blue, CFP axon) showing that the two distributions are not significantly different ( $P = 0.26$ , Kolmogorov–Smirnov test). **n**, Histograms showing axon diameters for all CFP (blue) and YFP (yellow) axon terminal branches are not significantly different ( $P = 0.54$ , Kolmogorov–Smirnov test). Scale bar, 10  $\mu\text{m}$ .

likely that the patterns or amounts of activity of the co-innervating motor axons are different<sup>16,17</sup>. If asynchronous synaptic activation of the postsynaptic cell is the principal mechanism driving competition forward, then the result should be identical on all post-synaptic cells co-innervated by the same axons.

This hypothesis implies the existence of one axon with the ‘best’ activity pattern that consequently maintains all of its branches and another axon with the ‘worst’ activity pattern that withdraws from the muscle completely, neither of which has been observed<sup>8,9</sup>. Alternatively, the relative competitive vigour of a neuron might depend both on the pattern of activity of its axon branches (which is fixed) and the efficacy of its synapses (which is malleable)<sup>18</sup>. Synaptic efficacy might, for example, be inversely related to the size of an axonal arbor. As an individual neuron withdraws at several post-synaptic target cells synchronously, it could subsequently redistribute synaptic resources to its remaining branches, increasing their competitive vigour and perhaps synchronously flipping the outcome in favour of inputs that were temporarily losing<sup>19</sup>. Conversely, axons that win numerous competitions early would

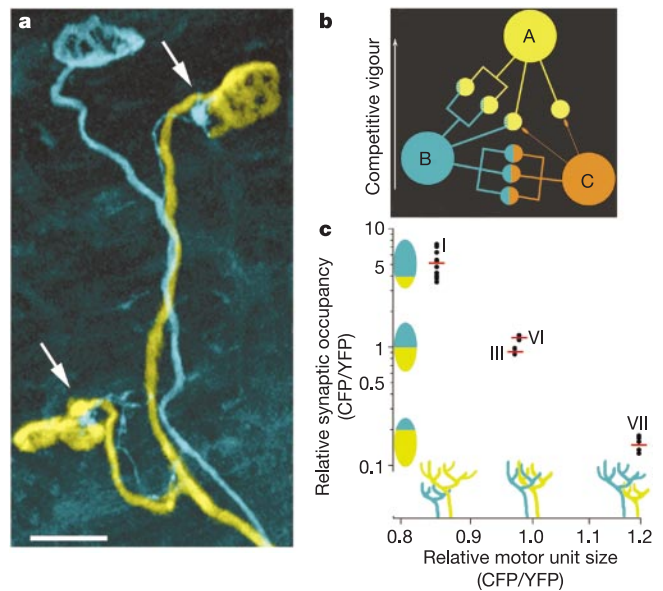


**Figure 4** The identity of neuronal competitors determines the outcome of synapse elimination. **a**, Two neuromuscular junctions (arrows) contacted by the same YFP (yellow) axon have recently lost input from the same CFP axon (muscle II, Fig. 2). In both cases (and a third co-innervated junction, not shown) the CFP axon, in the final stages of synapse elimination, has lifted off the junction surface. Scale bar, 20  $\mu\text{m}$ . **b**, Schematic of the connectivity of three motor units (A, B, C) showing the dominance of axon A over axon B, the similarity of axons B and C, and the dominance of A over C. These sets of interactions suggest a hierarchy in competitive vigour between the three axons (see Supplementary Fig. 2). **c**, Inverse relation between the skewing at individual co-innervated junctions and the relative sizes of the motor units of the two axons. Filled circles are individual neuromuscular junctions co-innervated by the two motor units (red lines, mean values; roman numerals refer to Fig. 2). Scale bar, 10  $\mu\text{m}$ .

commit resources to these fully occupied junctions, as a result weakening branches engaged in unresolved competitions. Finally, inputs initially highly divergent in competitive vigour might become more evenly matched by such readjustments in the pecking order, making the outcome of competition at some junctions more protracted than at others.

In summary, the surprising power of the identity of the neuronal competitors to determine the outcome and pace of synaptic competitions argues that some unique attribute of each neuron can affect the behaviour of its widely distributed branches. A reasonable candidate for this attribute is the potency of synaptic excitation by the individual branches, which in turn is determined by the number of action potentials in the parent axon and the amount of transmitter released from the terminal. In support of this notion, the accompanying paper<sup>4</sup> shows that decreasing synaptic efficacy strongly biases the outcome of competition at developing synapses. □

## Methods

### Mice

Transgenic mice (*thy1-YFP-H* and *thy1-CFP-S<sup>11</sup>*) were bred together to produce double-subset-expressing mice. Mice were mated to produce timed pregnancies, and the day of birth was considered postnatal day 0 (P0).

### Tissue preparation

Neonatal mice were deeply anaesthetized with sodium pentobarbital and perfused transcardially with 2% paraformaldehyde in 0.1 M phosphate buffered saline (PBS, pH 7.4). Forelimb muscles from both arms were dissected and post-fixed in 2% paraformaldehyde for 2 h. Muscles were rinsed in PBS, the connective tissue removed and the muscles were then incubated for 45 min in 5  $\mu\text{g} \mu\text{l}^{-1}$  Alexa-594-conjugated- $\alpha$ -bungarotoxin (Molecular Probes) diluted in 1% bovine serum albumin (BSA) in sterile lactated Ringer’s solution. After rinsing, muscles were mounted on slides in Vectashield (Vector Laboratories).

## Imaging and analysis

Motor units and neuromuscular junctions were reconstructed on laser scanning confocal microscopes (Olympus Flouview FV500 and Bio-Rad 1024). Images were obtained with a  $\times 60$  (1.4 NA) oil objective with a zoom equal to 2 for motor unit reconstructions and zoom equal to 4 for diffraction-limited imaging of individual junctions. YFP was excited with the 488 nm line of an argon laser and detected with a 520–550 nm band-pass emission filter. CFP was excited with the 442 nm line of an HeCd laser and detected with a 465–495 nm band-pass emission filter. Alexa-594  $\alpha$ -bungarotoxin was excited by using the 568 line of a Krypton laser and detected with a 585 long-pass barrier filter. Z-steps were 0.6  $\mu\text{m}$  for motor unit reconstructions and 0.3  $\mu\text{m}$  for high-resolution imaging of individual junctions.

Z-stacks were flattened by using a two-dimensional maximum projection algorithm in MetaMorph (Universal Imaging Corporation), and montages of the 20–50 stacks that constitute a motor unit were aligned with Adobe Photoshop. Percentage occupancy at individual junctions was determined in MetaMorph by counting the number of YFP (or CFP) pixels overlying receptors labelled with Alexa-594-conjugated  $\alpha$ -bungarotoxin. Axon diameter was determined, by using MetaMorph, as the width of the innervating CFP or YFP axon 10  $\mu\text{m}$  from the edge of the endplate where the axon enters. Branch number was determined by constructing complete branch diagrams of the motor units of interest and counting the number of branch points between the cell body and a particular junction.

Pair-wise statistical comparisons between motor units (i.e. CFP occupancy versus YFP occupancy) were done by using a non-parametric Mann–Whitney non-directional test. Distributions of histograms (Fig. 3 and Supplementary Fig. 1) were compared by using a Kolmogorov–Smirnov (K–S) goodness-of-fit test with S-Plus 4, MathSoft. We used a Monte Carlo simulation (column b, Fig. 2) to test whether the distribution of synaptic occupancy of a specific cohort of junctions facing the same competitor was different than the overall distribution of synaptic occupancy of the motor unit containing that cohort. As the most striking characteristic of the co-innervated junctions was their apparent similarity to each other, we compared the standard deviation of synaptic occupancy of junctions or axon diameter within the cohort with the standard deviation of the entire motor unit. Specifically, one trial of the Monte Carlo simulation randomly selected the same number of junctions from the entire motor unit as observed in the co-innervated cohort, and the standard deviation of that random sample was calculated (program written by S. Turney for Matlab). The process was repeated 100,000 times. The probability that the homogeneity occurring within a cohort could have occurred by chance was taken as the percentage of randomly selected samples that had an equal or smaller standard deviation than the cohort.

Received 5 February; accepted 2 June 2003; doi:10.1038/nature01836.

- Purves, D. & Lichtman, J. W. Elimination of synapses in the developing nervous system. *Science* **210**, 153–157 (1980).
- Wong, R. O. L. & Lichtman, J. W. in *Fundamental Neuroscience* (ed. Squire, L. et al.) 533–553 (Academic, San Diego, 2003).
- Keller-Peck, C. R. et al. Asynchronous synapse elimination in neonatal motor units: studies using GFP transgenic mice. *Neuron* **31**, 381–394 (2001).
- Buffelli, M. et al. Genetic evidence that relative synaptic efficacy biases the outcome of synaptic competition. *Nature*, this issue (2003).
- Lichtman, J. W. The reorganization of synaptic connections in the rat submandibular ganglion during post-natal development. *J. Physiol. (Lond.)* **273**, 155–177 (1977).
- Colman, H., Nabekura, J. & Lichtman, J. W. Alterations in synaptic strength preceding axon withdrawal. *Science* **275**, 356–361 (1997).
- Chen, C. & Regehr, W. G. Developmental remodeling of the retinogeniculate synapse. *Neuron* **28**, 955–966 (2000).
- Brown, M. C., Jansen, J. K. & Van Essen, D. C. Polyneuronal innervation of skeletal muscle in newborn rats and its elimination during maturation. *J. Physiol. (Lond.)* **261**, 387–422 (1976).
- Jansen, J. K. & Fladby, T. The perinatal reorganization of the innervation of skeletal muscle in mammals. *Prog. Neurobiol.* **34**, 39–90 (1990).
- Sanes, J. R. & Lichtman, J. W. Development of the vertebrate neuromuscular junction. *Annu. Rev. Neurosci.* **22**, 389–442 (1999).
- Feng, G. et al. Imaging neuronal subsets in transgenic mice expressing multiple spectral variants of GFP. *Neuron* **28**, 41–51 (2000).
- Press, W. H., Teukolsky, S. A., Vetterling, W. T. & Flannery, B. P. *Numerical Recipes in C* (Cambridge Univ. Press, 1992).
- Gan, W. B. & Lichtman, J. W. Synaptic segregation at the developing neuromuscular junction. *Science* **282**, 1508–1511 (1998).
- Personius, K. E. & Balice-Gordon, R. J. Activity-dependent editing of neuromuscular synaptic connections. *Brain Res. Bull.* **53**, 513–522 (2000).
- Balice-Gordon, R. J. & Lichtman, J. W. Long-term synapse loss induced by focal blockade of postsynaptic receptors. *Nature* **372**, 519–524 (1994).
- Buffelli, M., Busetto, G., Cangiano, L. & Cangiano, A. Perinatal switch from synchronous to asynchronous activity of motoneurons: link with synapse elimination. *Proc. Natl Acad. Sci. USA* **99**, 13200–13205 (2002).
- Personius, K. E. & Balice-Gordon, R. J. Loss of correlated motor neuron activity during synaptic competition at developing neuromuscular synapses. *Neuron* **31**, 395–408 (2001).
- Barber, M. J. & Lichtman, J. W. Activity-driven synapse elimination leads paradoxically to domination by inactive neurons. *J. Neurosci.* **19**, 9975–9985 (1999).
- Walsh, M. K. & Lichtman, J. W. In vivo time lapse imaging of synaptic takeover associated with naturally occurring synapse elimination. *Neuron* **37**, 1–7 (2003).

Supplementary Information accompanies the paper on [www.nature.com/nature](http://www.nature.com/nature).

**Acknowledgements** We thank the members of our laboratory and J. R. Sanes for many useful discussions, J. Tollet for help breeding animals, J. D. Wiley for assistance in collecting initial data, and S. Turney for technical advice and developing programs for the statistical tests. We thank J. R. Sanes and G. Feng for generating the original transgenic mice. This work was supported by grants from the National Institutes of Health and the Muscular Dystrophy Association to J.W.L., and by support from the Bakewell Neuroimaging Fund.

**Competing interests statement** The authors declare that they have no competing financial interests.

**Correspondence** and requests for materials should be addressed to J.W.L. (jeff@pcg.wustl.edu).

## Genetic evidence that relative synaptic efficacy biases the outcome of synaptic competition

Mario Buffelli\*<sup>†</sup>, Robert W. Burgess\*<sup>‡</sup>, Guoping Feng\*<sup>‡</sup>,  
Corrinne G. Lobe<sup>§</sup>, Jeff W. Lichtman\* & Joshua R. Sanes\*

\* Department of Anatomy and Neurobiology, Washington University School of Medicine, 660 South Euclid, St Louis, Missouri 63110, USA

† Dipartimento di Scienze Neurologiche e della Visione, Università degli Studi di Verona, Via dell' Artiglierie 8, 37129 Verona, Italy

§ Sunnybrook and Women's College Health Science Centre, 2075 Bayview, Toronto, Ontario M4N 3M5, Canada

Synaptic activity drives synaptic rearrangement in the vertebrate nervous system; indeed, this appears to be a main way in which experience shapes neural connectivity<sup>1,2</sup>. One rearrangement that occurs in many parts of the nervous system during early post-natal life is a competitive process called 'synapse elimination'<sup>3,4</sup>. At the neuromuscular junction, where synapse elimination has been analysed in detail, muscle fibres are initially innervated by multiple axons, then all but one are withdrawn and the 'winner' enlarges<sup>4–6</sup>. In support of the idea that synapse elimination is activity dependent, it is slowed or speeded when total neuromuscular activity is decreased or increased, respectively<sup>4,7–13</sup>. However, most hypotheses about synaptic rearrangement postulate that change depends less on total activity than on the relative activity of the competitors<sup>1–4,13,14</sup>. Intuitively, it seems that the input best able to excite its postsynaptic target would be most likely to win the competition, but some theories and results make other predictions<sup>14–18</sup>. Here we use a genetic method to selectively inhibit neurotransmission from one of two inputs to a single target cell. We show that more powerful inputs are strongly favoured competitors during synapse elimination.

The only two experiments that have differentially decreased activity of some inputs to a muscle led to opposite conclusions: the more active axon was favoured in one, and the less active in the other<sup>17,18</sup>. To re-examine this issue, we reduced neurotransmission from a subset of motor axons by depleting them of choline acetyltransferase (ChAT), the sole synthetic enzyme for the neurotransmitter, acetylcholine. Neuromuscular junctions (NMJs) form in mutant mice that completely lack ChAT (*ChAT*<sup>−/−</sup>), but electrophysiological recordings showed that no neurotransmission occurs, and the mice die at birth<sup>19,20</sup>. Here, we used a conditional allele of the *ChAT* gene (*ChAT*<sup>lox/lox</sup>), so that we could allow embryogenesis to proceed normally, then inactivate *ChAT* postnatally. Exons near the 5' end of ChAT were flanked by loxP sites; excision by Cre recombinase generated the *ChAT*<sup>−/−</sup> allele<sup>19</sup>. To

‡ Present addresses: Jackson Laboratories, Bar Harbor, Maine 04609, USA (R.W.B.); Department of Neurobiology, Duke University Medical School, Durham, North Carolina 27710, USA (G.F.).